Electronic Supplementary Information

Facile synthesis of MoS_2/graphene composites: effects of different cationic surfactants on microstructures and electrochemical properties of reversible lithium storage

Zhen Wang,[a] Lin Ma,[a] Weixiang Chen,*[a] Guochuang Huang,[a] Dongyun Chen,[b] Lianbang Wang,[c] Jim Yang Lee[b]

[a] *Department of Chemistry, Zhejiang University, Hangzhou 310027, China.*
Fax: +86 571 87951895; Tel: +86 571 87952477; E-mail: weixiangchen@zju.edu.cn

[b] *Department of Chemical and Biomolecular Engineering, National University of Singapore, 10 Kent Ridge Crescent, 119260, Singapore*

[c] *Collage of Chemical Engineering and Materials Science, Zhejiang University of Technology, Hangzhou 310014, China*

As shown Table 1, the carbon contents in the three composite samples (MoS_2/GNS-D, MoS_2/GNS-O and MoS_2/GNS-T) are different, respectively. In general, the different carbon contents of the composites will have different effects on the electrochemical performance of the anode materials for reversible lithium storage. In order to exclude the influence of the carbon content in the MoS_2/GNS composites, other two composites (MoS_2/GNS-S1 and MoS_2/GNS-S2) were synthesized by same liquid phase chemical reduction route and heat treatment. The carbon content of the MoS_2/GNS-S1 (or MoS_2/GNS-S2) composite was controlled to be very close (or almost equal) to that of MoS_2/GNS-D (or MoS_2/GNS-O) by changing the amounts (or ratios) of starting materials. The amounts of starting materials are shown in Table S1. The microstructure and element composition of MoS_2/GNS-S1 and MoS_2/GNS-S2 composites were characterized by X-ray diffraction (XRD, D8 ADVANCE X-ray diffractometer with Cu Kα radiation λ=0.15405 nm), transmission electron microscopy (TEM, JEOL JEM-200CX microscope operating at an acceleration voltage of 200 kV), high resolution transmission electron microscopy (HRTEM) and energy dispersive X-ray spectroscopy (EDX, GENENIS-4000). Electrochemical performances of MoS_2/GNS-S1 and MoS_2/GNS-S2 composites were tested using two-electrode coin cells (CR2025) by galvanostatic charge/discharge cycling between the voltage limits of 0.005 and 3.0 V on a LANHE 2001A Battery Tester.

Table S1 The amounts of starting materials for preparing MoS_2/GNS-S1 and MoS_2/GNS-S2 composites

Composites	GOS /mmol	Surfactant	$(NH_4)_2MoS_4$ /mmol
MoS_2/GNS-S1	8.07	100 mL of 0.01 M DTAB solution	2.69
MoS_2/GNS-S2	9.42	No using	2.69

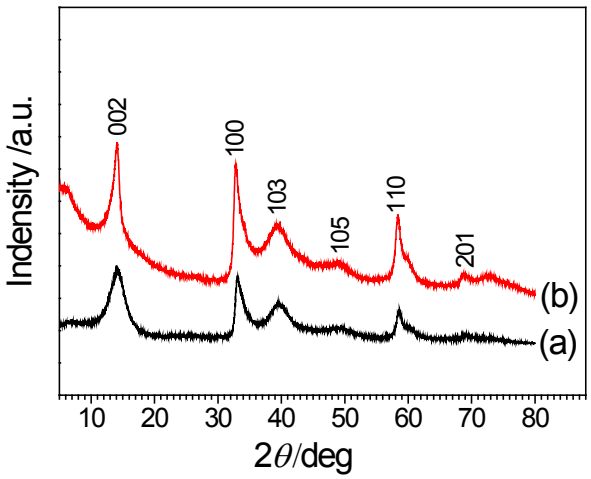

Fig. S1 XRD patterns of (a) MoS_2/GNS-S1 and (b) MoS_2/GNS-S2 composites

XRD patterns of MoS_2/GNS-S1 and MoS_2/GNS-S2 composites are shown in Fig. S1. Both MoS_2/GNS-S1 and MoS_2/GNS-S2 composites clearly displays diffraction peaks of MoS_2, which can be indexed to the (002), (100), (103), (105), (110) and (201) planes of the 2H-MoS_2 (JCPDS card No. 37-1492), respectively. For both composites, the interlayer space $d_{(002)}$ of MoS_2 is calculated to be 0.62 nm according to the (002) peak at 2θ=14.17°. As shown in Fig. S1, MoS_2/GNS-S1 displays broadening and lower (002) reflection compared to MoS_2/GNS-S2, indicating the layer number of MoS_2 in MoS_2/GNS-S1 is less than that in MoS_2/GNS-S2.

Fig. S2 shows the TEM/HRTEM images of MoS_2/GNS-S1 and MoS_2/GNS-S2 composites. As shown in Fig. S2(a, b), MoS_2/GNS-S1 displays that few-layer MoS_2 sheets (3~5 layer) dispersed on the wrinkled graphene surface can be clearly found. Fig. S2(c, d) shows that for MoS_2/GNS-S2 composite, the layered MoS_2 sheets (about 7~11 layer) supported on the wrinkled graphene surface can also be found. HRTEM images of MoS_2/GNS-S1 and MoS_2/GNS-S2 composites clearly show the few-layered or layered MoS_2 structure with $d_{(002)}$ of 0.62 nm, which agree with their XRD analysis.

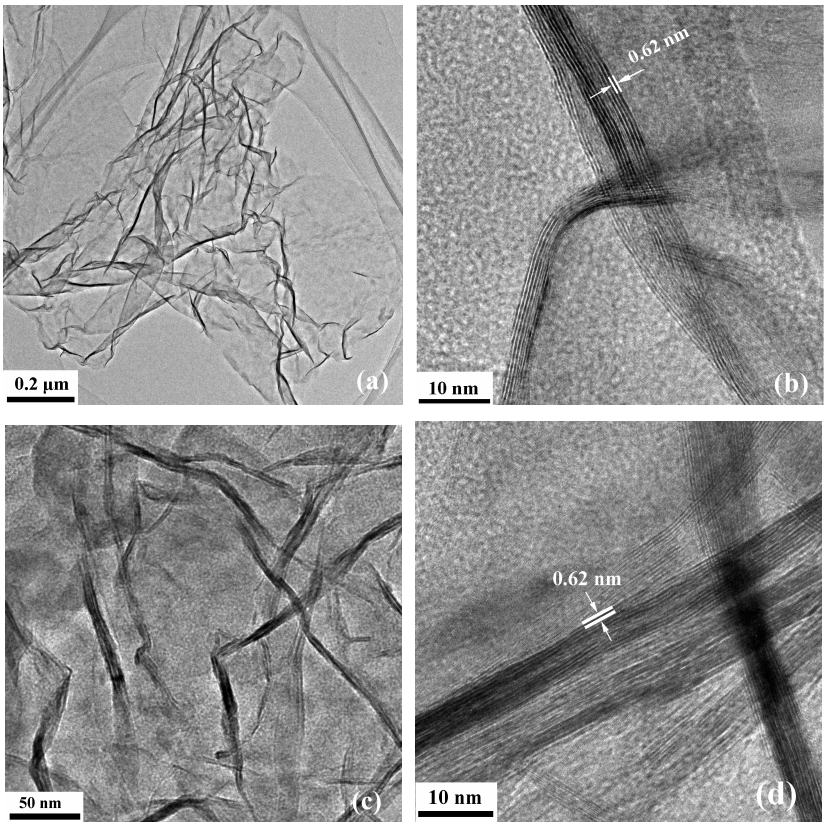

Fig. S2 TEM/HRTEM images of (a, b) MoS_2/GNS-S1 and (c, d) MoS_2/GNS-S2 composites.

Table S2 Elemental compositions of MoS_2/GNS-S1 and MoS_2/GNS-S2 composites (S: Mo represents the atomic ratio)

Composites	C /wt%	O /wt%	Mo /wt%	S /wt%	MoS_2 /wt%	S:Mo
MoS_2/GNS-S1	26.95	8.51	38.91	25.63	64.54	1.97
MoS_2/GNS-S2	21.63	5.32	43.45	29.60	73.05	2.04

The elemental compositions of MoS_2/GNS-S1 and MoS_2/GNS-S2 were examined by EDX as summarized in Table S2. The atomic ratios of S to Mo calculated for both samples are very approaching to the stoichiometry of MoS_2. The strong presences of C in the composites are clearly derived from the reduced GO and amorphous carbon from the carbonization of the surfactant (DTAB). A small amount of O should be provided by residual oxygenic functional groups of reduced GO and amorphous carbon. As shown in Table S2, the content of MoS_2/GNS-S1 is 26.95 *wt*%, which is very close to that (26.29 *wt*%) of MoS_2/GNS-D composite. The content of MoS_2/GNS-S2 is 21.63 *wt*%%, which is almost equal to that (21.32 *wt*%%) of MoS_2/GNS-O composite.

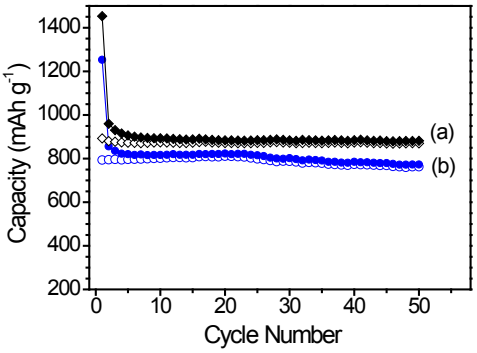

Fig. S3 Cycling performances of (a) MoS_2/GNS-1 and (b) MoS_2/GNS-2 composites at a current density of 100 mA g^{-1}.

Fig. S3 shows the cycling performances of MoS_2/GNS-S1 and MoS_2/GNS-S2 composites at a constant current density of 100 mA g^{-1}. At the first cycle, the lithiation capacity is 1453 and 1253 mAh g^{-1} for MoS_2/GNS-S1 and MoS_2/GNS-S2 composite, respectively. The corresponding reversible capacity is 892 and 793 mAh g^{-1} with the Columbic efficiencies of 61.4% and 63.3%. The irreversibility in the first cycle is due to the irreversible electrode process such as the formation of the SEI film, the electrochemically driven electrolyte degradation, reduction of oxygen-containing groups and being trapped of a small amount of lithium in the defect sites or disordered structures. As shown in Fig. S3, both MoS_2/GNS-S1 and MoS_2/GNS-S2 composite electrodes exhibit stable cycling performance. After 50 cycles, MoS_2/GNS-S1 and MoS_2/GNS-S2 composite electrodes remain the reversible capacity of 869 and 762 mAh g^{-1}, respectively.

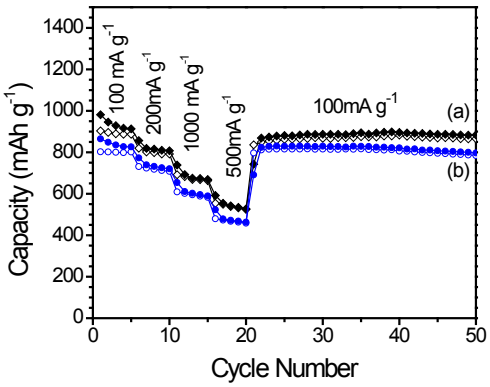

Fig. S4 Rate capability of (a) MoS_2/GNS-S1 and (b) MoS_2/GNS-S2 composites at different charging/discharging current densities.

Fig. S4 shows the rate capability of MoS_2/GNS-S1 and MoS_2/GNS-S2 composites at the different charging/discharging current densities. At a high current density of 1000 mA g^{-1}, the reversible capacity of MoS_2/GNS-S1 and MoS_2/GNS-S2 electrodes is 549-524 mAh g^{-1} and 472-458 mAh g^{-1}, respectively.

The electrochemical performances comparison of MoS_2/GNS-S1 and MoS_2/GNS-D, MoS_2/GNS-S2 and MoS_2/GNS-O for reversible lithium storage are summarized in Table S3. As listed in Table S3, even if the carbon content of MoS_2/GNS-S1 is very close to that of MoS_2/GNS-D composite, MoS_2/GNS-S1 exhibits lower reversible capacity and poor rate capability than MoS_2/GNS-D composite. In particular, the carbon content of MoS_2/GNS-S2 is almost equal to that of MoS_2/GNS-O composite, but MoS_2/GNS-S2 exhibits much lower reversible capacity and poor rate capability in comparison with MoS_2/GNS-D composite. Therefore, the factor of the carbon content in the composites can be excluded.

Table S3 Electrochemical performance comparison of MoS_2/GNS-S1, MoS_2/GNS-D, MoS_2/GNS-S2 and MoS_2/GNS-O for reversible lithium storage

Composites	Carbon content /wt%	Cycling performance	Reversible capacity at 100 mA g^{-1} （mAh g^{-1}）	Rate-capability at 1000 mA g^{-1} （mAh g^{-1}）
MoS_2/GNS-S1	26.95	Excellent	~893	549-524
MoS_2/GNS-D	26.29	Excellent	~932	676-657
MoS_2/GNS-S2	21.63	Good	~793	472-458
MoS_2/GNS-O	21.32	Excellent	~1050	731-716